WORKSHOP
Direct and Large-Eddy Simulation 13
October 26th-29th 2022, Udine, Italy

SIMULATION OF MASSIVELY SEPARATED FLOWS USING HYBRID TURBULENCE MODELS AND MESH ADAPTATION

F. Miralles[1], B. Sauvage[2], S. Wornom[1], F. Alauzet[3], B. Koobus[1] and A. Dervieux [2,4]
[1] IMAG, Univ. Montpellier, CNRS, France, florian.miralles@umontpellier.fr, bruno.koobus@umontpellier.fr, stephen.wornom@inria.fr
[2] Université Côte d'Azur, INRIA Sophia-Antipolis, France, bastien.sauvage@inria.fr, alain.dervieux@inria.fr
[3] INRIA Saclay, France, frederic.alauzet@inria.fr
[4] Lemma, Biot, France, alain.dervieux@inria.fr

INTRODUCTION

The simulation of unsteady flows characterized by large separations induced by adverse pressure gradient is still a challenge at high Reynolds numbers. For such simulations, hybrid models are those favored due to the cost/accuracy compromise they offer. In this study, we assess, next to the DDES approach, the performance of two hybrid models for the prediction of the flow around a circular cylinder at Reynolds numbers 10^6 and 2×10^6, and the flow over a NACA0021 airfoil in a deep stall at Reynolds number 270000. These hybrid models combine either a RANS model or the DDES approach with the dynamic variational multiscale (DVMS) model for the large eddy simulation. A mesh adaptation procedure is currently being applied for the NACA0021 benchmark, with the aim of improving the prediction of the aerodynamic and aeroacoustic characteristics of the flow, such as the airfoil self-noise generation and propagation.

TURBULENCE MODELING

We start by briefly specifying the base ingredients of our hybrid turbulence strategies, namely the RANS or DDES component, and the DVMS component.

• **RANS component**: two low Reynolds RANS models are used in our hybrid models, more specifically they are the $k-\varepsilon$ model proposed in Goldberg et al.[1] and the $k-R$ model recently introduced in [2] by Zhang et al. They have been chosen for their abilities to properly predict separated flows with adverse pressure gradients.

• **DDES component**: in this work, the classical DDES approach [3] is based either on the Spalart-Allmaras model or the $k-\varepsilon$ model of Goldberg [1].

• **LES-like component**: the DVMS approach proposed in [4] is used as the LES part of our hybrid models. In this approach, the variational multiscale (VMS) model, aiming to limit the effects of the subgrid-scale (SGS) model to the smallest resolved scales, is combined with the dynamic procedure which provides a tuning of the SGS dissipation in space and time, so that the resulting DVMS model enjoys synergistic effects. An important consequence is that the DVMS model introduces less dissipation than its LES counterpart (based on the same SGS model).

• **Hybrid models** Our hybrid strategies blend either a RANS or DDES model with the DVMS approach [5]. After semi-discretization, these hybrid models can be written as

$$\left(\frac{\partial W_h}{\partial t},\Phi_i\right)+(\nabla\cdot F(W_h),\Phi_i)= -\theta\left(\tau^{\mathrm{mod}}(W_h),\Phi_i\right)-(1-\theta)\left(\tau^{\mathrm{DVMS}}(W_h'),\Phi_i'\right) \quad (1)$$

where the stress tensor τ^{mod} holds for either the RANS stress tensor or the stress tensor used in the DDES approach based on a given RANS model, τ^{DVMS} is the SGS term that applies in DVMS on the small resolved scales component W_h' of the hybrid variable W_h, Φ_i denotes the basis and test functions, F denotes the convective and viscous fluxes, and θ is the blending function.

Two blending functions are applied in this work, which allow an automatic and progressive switch from RANS or DDES to DVMS where the grid resolution is fine enough to resolve a significant part of the local turbulence scales or fluctuations. Typically, it is desirable to have the DVMS component activated in the wake region instead of the RANS or DDES component due to the low dissipation introduced by the DVMS approach. Additionally, these blending functions prevent the activation of the DVMS mode in the boundary layer through the use of a shielding function. These blending functions can write as $\theta=1-f_d(1-\tanh(\xi^2))$ with $\xi=\frac{\Delta}{l_{RANS}}$ where l_{RANS} denotes the characteristic RANS scale, Δ is the filter width, and f_d is a shielding function which characterizes each of the two blending functions applied in this work:

∘ $f_d=f_{\mathrm{ddes}}$ the delaying function used in DDES (see [3])

∘ $f_d=f_{\mathrm{geo}}=\exp\left(-\frac{1}{\epsilon}\min^2(d-\delta_0,0)\right)$ with d the normal distance to the wall, $\epsilon>0$ small enough and $\delta_0>0$ (of the order of the boundary layer thickness).

NUMERICAL MODEL

The spatial discretization, detailed in [4, 5] is an upwing finite-volume/finite element of low dissipation (sixth-order space derivatives). A novelty is the combination with the Transient Fixed Point mesh adaptation loop of [6].

APPLICATIONS

• **Flow past a cylinder** Two Reynolds numbers, 10^6 and 2×10^6, based on the cylinder diameter and on the freestream velocity, are considered. From Table 1, it can be noted that

the prediction of these coefficients by the hybrid simulations at Reynolds number 10^6 are globally in good agreement with the experimental data. The distribution over the cylinder surface of the mean pressure coefficient, shown in Figure 1, confirms this trend. The same observations can be made at Reynolds number 2×10^6 (results not shown for the sake of brevity).

• **Flow over an airfoil in a deep stall** A NACA0021 airfoil at an angle of attack 60^o is considered at Reynolds number 270000 based on the chord length. A coarse mesh of 517 K vertices is used. Two bulk coefficients and the distribution of the mean pressure coefficient over the airfoil surface are respectively given in Table 2 and Figure 3 as an example. Ongoing results using an adapted mesh (Figure 2), as well as acoustic post-processing, will also be shown.

REFERENCES

[1]Goldberg, U., Peroomian, O. and Chakravarthy, S. : A wall-distance-free $k-\varepsilon$ model with Enhanced Near-Wall Treatment, *Journal of Fluids Engineering*, **120**, 457–462 (1998).

[2]Zhang, Y., Rahman, M.M. and Chen, G. : Development of k-R turbulence model for wall-bounded flows, *Aerospace Science and Technology*, **98** (2020).

[3]Spalart, P., Deck, S., Shur, M., Squires, S., Strelets, M., and Travin, A. A new version of detached-eddy simulation, resistant to ambiguous grid densities. *Theory and Computational Fluid Dynamics*, 20:181–195, 2006.

[4]Moussaed, C., Wornom, S., Salvetti, M.V., Koobus, B. and Dervieux, A. : Impact of dynamic subgrid-scale modeling in variational multiscale large-eddy simulation of bluff body flows, *Acta Mechanica*, **225**, 3309-3323 (2014).

[5]Moussaed, C., Salvetti, M.V., Wornom S., Koobus, B. and Dervieux, A. : Simulation of the flow past a circular cylinder in the supercritical regime by blending RANS and variational-multiscale LES models, *Journal of Fluids and Structures*, **47**, 114-123 (2014).

[6]Alauzet, F., Frey, P.J., George, P.-L., and Mohammadi, B.. 3D transient fixed point mesh adaptation for time-dependent problems: Application to CFD simulations. *J. Comp. Phys.*, 222:592–623, 2007.

	$\overline{C}_d$	C'_l	$-\overline{C}_{pb}$	$\overline{\theta}$
Present simulations				
DDES	0.20	0.04	0.22	138
DDES/DVMS (f_{ddes})	0.20	0.02	0.22	135
RANS/DVMS (f_{ddes})	0.25	0.09	0.25	132
Measurements				
Exp. Shih et al. (1993)	-	0.24	0.33	-
Exp. Szechenyi (1975)	0.25	0.32	-	-
Exp. Goelling (2006)	-	-	-	130

Table 1: Bulk coefficients of the flow around a circular cylinder at Reynolds number $\mathbf{10^6}$. $\overline{C}_d$ denotes the mean drag coefficient, C'_l the root mean square of lift time fluctuations, $\overline{C}_{p_b}$ the mean pressure coefficient at cylinder basis, and $\overline{\theta}$ the mean separation angle.

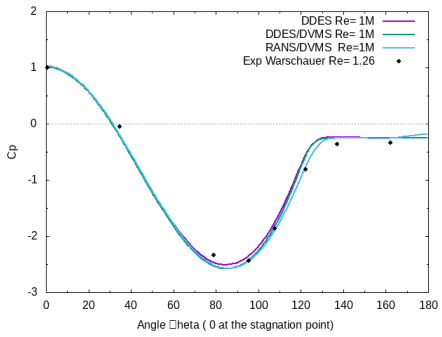

Figure 1: Distribution over the cylinder surface of the mean pressure coefficient at Reynods number $\mathbf{10^6}$.

	Mesh size	$\overline{C}_d$	$\overline{C}_l$
Present simulations			
RANS/DVMS (f_{dgeo})	0.5M	1.66	1.03
RANS/DVMS (f_{ddes})	0.5M	1.54	0.95
DDES/DVMS (f_{geo})	0.5M	1.77	1.06
DDES/DVMS (f_{ddes})	0.5M	1.64	1.01
DDES-SA/mesh adaptation	0.2M	1.53	0.97
Measurement			
Exp. Swalwell (2005)		1.517	0.931

Table 2: Mean drag and lift coefficients for the NACA0021.

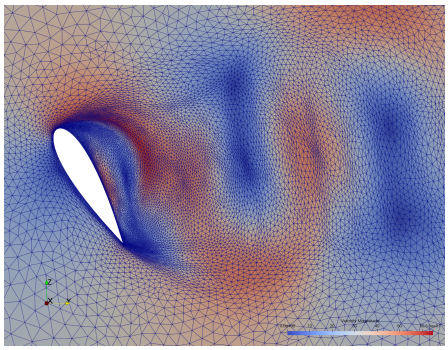

Figure 2: Partial view of a 0.9M adapted mesh and velocity $0 \leq ||U|| \leq 65$.

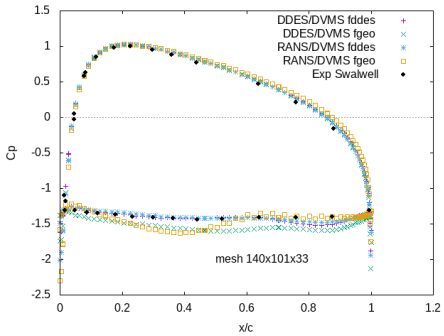

Figure 3: Mean pressure coefficient over the airfoil surface.